dioxygen, reacting so rapidly that the electronic spectrum must be obtained under rigorously anaerobic conditions. [Fe(TTP)NO] and [Fe(OEP)NO] are somewhat more resistant to oxidation. When the reaction with dry dioxygen is carried out in sealed reaction vessels, all three porphyrin species yield primarily [Fe(P)NO_3]. Only μ-oxo derivatives are found when the reaction is allowed to proceed in an open vessel. The addition of either a Lewis base (pyridine) or a Lewis acid (BF_3·Et_2O) significantly increases the stability of the complexes toward dioxygen. Reaction with iodosobenzene was sluggish, and significant amounts of new porphyrinic products were only obtained with excess (20-fold) iodosobenzene. Products in toluene were starting complex, [Fe(TPP)NO_3], and [Fe(TPP)]$_2$O. *N*,*N*-Dimethylaniline *N*-oxide, a slightly milder oxidant than iodosobenzene, gave no reaction in toluene, dichloromethane, or THF. There was no evidence for the formation of nitrite complexes in any of these sysems.

The conversion of the nitrite complex to a nitrosyl complex is directly analogous to the first step in the catalytic cycle of assimilatory nitrite reductase. Conversions of this type have been observed in other nitrite complexes.[33] Our results suggest that this conversion is an intrinsic property of heme nitrite complexes. If this is the case, such a conversion requires no active participation of an enzyme. The role of the enzyme may be that of control rather than performance in this conversion reaction. Our observation of the instability of the nitrite complex along with the observation of Barley et al.[33] of rapid reduction of ammonia following the reduction of the [Fe(TPP)NO]$^-$ species indicates that the nitrosyl complexes are the most stable complexes in this series. All that is required for the formation of the nitrosyl complex is an accepter for an oxygen atom. Nitrite ion apparently fits this description, although the enzymatic systems may well have other oxygen acceptors available.

As noted earlier, Fernandes et al.[9] have previously reported the preparation of a nitrite complex of (tetraphenylporphyrinato)iron(III). This report makes no mention of decomposition of the nitrite complex to a nitrosyl derivative, although nitric oxide and nitrosyl complexes were noted in subsequent electrochemical analysis of solutions containing the nitrite complex. The electronic spectrum in DMF of the complex that Fernandes et al. characterize as a bis(nitrite) complex is similar to that of complex **1** we reported (Table I). The spectral characteristics in dichloromethane solution that Fernandes et al.[9] assign to the bis(nitrite) complex are close to those that we have found for the nitrosyl–nitrito complex (Table I). Neither of the two spectra are close to that of a bona fide bis(nitrite) sample prepared with picket-fence porphyrin[24] and whose spectra display almost no solvent dependence (Table I). (It should be noted that picket-fence porphyrin and TPP derivatives have quite similar spectral properties.) We are also intrigued by the report of their difficulties with the formation of the μ-oxo species in dichloromethane but not in DMF. In our hands, the formation of a μ-oxo complex due to residual water was much more facile in DMF than in dichloromethane. Their detection of nitrosyl complexes during cyclic voltametry of solutions containing nitrite and porphyrin may be due to electrochemical reduction of the nitrite complex or to the reaction we have described. The conversion of nitrite complexes to nitrosyl complexes in the presence of excess nitrite presents a caveat for the interpretation of spectra of solutions containing porphyrins and nitrite. Such spectra are likely to be complicated by the production of nitrosyl and/or nitrosyl–nitrite complexes. This is particularly true if the solutions used are not freshly prepared or if the acquisition time of the experimental technique is relative long (such as standard FT-NMR techniques).

Concluding Remarks. Our spectroscopic and kinetic data for the nitrite/(porphinato)iron(III) system are consistent with nitrite ion behaving as a relatively strongly binding ligand toward iron(III) porphyrinates. Nitrite clearly displaces weakly bound ligands such as perchlorate or nitrate. The resulting nitrite complex interacts with excess nitrite ion to produce a nitrosyl complex. The other product of this oxygen atom transfer reactions is most likely nitrate ion. We thus find that the nitrite complex of iron(III) porphyrin has limited stability. The intermolecular reaction that we postulate also suggests appropriate synthetic strategies that could be used to prepare stable nitrite complexes. This question is considered in the following paper.[24]

Note Added in Proof. Prof K. S. Suslick has recently prepared a manganese(III) porphyrinate having an O-bonded nitrite ion: Suslick, K. S. Personal communication. Suslick, K. S.; Watson, R. A. *J. Inorg. Biochem.* **1988**, *36*, Abstract L032.

Acknowledgment. We thank the National Institutes of Health for support of this research under Grant GM-38401. We also thank Dr. J. Fajer for a helpful discussion concerning nitro oxygen atom transfer reactions.

(33) (a) Godwin, J. B.; Meyer, T. J. *Inorg. Chem.* **1971**, *10*, 2150. (b) Murphy, W. R., Jr.; Takeuchi, K. J.; Meyer, T. J. *J. Am. Chem. Soc.* **1982**, *104*, 5817. (c) Murphy, W. R., Jr.; Takeuchi, K.; Barley, M. H.; Meyer, T. J. *Inorg. Chem.* **1986**, *25*, 1041.

Contribution from the Department of Chemistry and Biochemistry, University of Notre Dame, Notre Dame, Indiana 46556

Use of Protected Binding Sites for Nitrite Binding in Iron(III) Porphyrinates. Crystal Structure of the Bis(nitro)($\alpha,\alpha,\alpha,\alpha$-tetrakis(*o*-pivalamidophenyl)porphinato)iron(III) Anion

Habib Nasri, John A. Goodwin, and W. Robert Scheidt*

Received February 28, 1989

The reaction of nitrite ion with iron(III) picket-fence porphyrin species leads to the synthesis of low-spin bis(nitro) complexes. These compounds have been characterized by EPR, IR, UV–vis, and NMR spectroscopy. The crystal structure of one derivative, [K(18-C-6)(H_2O)][Fe(NO_2)$_2$(TpivPP)], has been determined. The complex has one N-bound nitrite within the ligand-binding pocket of the pickets; the other N-bound nitrite is on the open side of the porphyrin plane but is protected from reaction by the formation of a tight ion pair with the [K(18-C-6)(H_2O)]$^+$ cation: there are two K–O(NO_2) bonds = 2.9 Å. Equatorial Fe–N bond distances average to 1.992 (1) Å while the axial Fe–N distances average to 1.985 (22) Å. Crystal data: tetragonal system, $FeKO_{15}N_{10}C_{76}H_{90}$, space group $P\bar{4}$, a = 16.691 (6) Å, c = 13.534 (3) Å, Z = 2. A total of 4184 observed data were used in the structure solution and refinement with final values of $R(F_o)$ = 0.069 and $R_w(F_o)$ = 0.066. Ligand-binding studies, followed by NMR or EPR spectroscopy, were performed in an attempt to assign the spin state of the intermediate mono(nitro) complex, which appears to be a high-spin species. Association constants for the formation of mono- and bis(nitrite) complexes are reported; differences as a function of counterion are consistent with significant ion-pairing differences.

In the preceding paper,[1] we described the reactions of the (porphinato)iron(III)/nitrite system that apparently prevented the isolation of nitro(porphinato)iron(III) complexes. These reactions appear to involve attack on the coordinated nitrite ion to

0020-1669/90/1329-0185$02.50/0

yield, inter alia, iron nitrosyl species. We report in this paper the results of the reaction of nitrite ion with (porphinato)iron(III) species having a protected ligand-binding site. We have used the now well-known "picket-fence" porphyrin strategy, first described by Collman et al.[2] Reactions of iron(III) picket-fence porphyrin with nitrite salts afford nitrite-ligated derivatives. These bis(nitro) low-spin complexes have been characterized by UV–vis, IR, NMR, and EPR spectroscopy. One complex has also been characterized by a single-crystal X-ray structure determination. The stepwise ligand-binding constants have been measured. Interestingly, the long-term solution stability of these nitrite derivatives is dependent on the identity of the counterion. The probable basis for this counterion effect is found from the crystal structure analysis of the complex studied, hereinafter abbreviated as $[K(18\text{-}C\text{-}6)(H_2O)][Fe(NO_2)_2(TpivPP)]$.[3] The crystal structure shows that the potassium(18-crown-6) cation forms a tight ion pair through an interaction of the K^+ ion with the two oxygen atoms of the nitrite ion on the "open" face of the porphyrin complex. The reactivity patterns of these picket-fence derivatives are entirely consistent with the results of the previous paper.

Experimental Section

Synthesis of $[K(18\text{-}C\text{-}6)(H_2O)][Fe(NO_2)_2(TpivPP)]$. $[Fe(SO_3CF_3)(H_2O)(TpivPP)]$[4] (100 mg, 0.08 mmol), 18-crown-6 (210 mg, 0.79 mmol), and KNO_2 (100 mg, 1.118 mol) in 15 mL of chlorobenzene (dried by distillation from P_2O_5) were stirred for 3 h at room temperature. This deep red solution was then filtered, and single crystals of the complex were prepared by slow diffusion of pentane into the chlorobenzene solution. The resulting crystalline material was washed with portions of distilled water to remove excess ligand and then washed with several portions of dry pentane. Typical yields were 70–80%. UV [λ_{max} in chlorobenzene (log ϵ)]: 364 (sh, 4.52), 425.5 (5.11), 464 (sh, 4.40), 553 (4.15) nm. IR (KBr pellet): $\nu(NO_2)$ 1351 (s), 1315 (s) cm^{-1}. EPR (solid state, 77 K): $g_1 = 2.722$, $g_2 = 2.522$, and $g_3 = 1.575$. Chlorobenzene solutions (77 K) gave the same EPR spectrum. ^1H NMR [$\delta(H_{pyrrole})$ in $CDCl_3$]: −14.5 ppm.

The anionic species was also prepared by using cryptand 222 as the solubilizing agent for nitrite and by using Ph_4PNO_2. The Ph_4P^+ salt gave essentially the same UV–vis and EPR spectra but slightly different NMR spectra ($H_{pyrrole}$ resonance at −15.7 ppm).

Ligand-Binding Studies. Spectrophotometric titrations of $[Fe(SO_3CF_3)(H_2O)(TpivPP)]$ with NO_2^- were carried out in dichloromethane and chlorobenzene by addition of concentrated solutions of NO_2^- to solutions of $[Fe(SO_3CF_3)(H_2O)(TpivPP)]$ in a 10-mL flask with a 1-mm side-arm cuvette sealled with a Teflon-lined spectrum. The added solutions contained $[Fe(SO_3CF_3)(H_2O)(TpivPP)]$ at the same concentration as the solution in the flask in order to maintain a constant (porphinato)iron(III) concentration. Ionic strength was not controlled so as to avoid competitive binding of the anion of the ionic strength medium. All additions were made by Hamilton microliter syringe. All spectrophotometric measurements were made with a Perkin-Elmer Lambda 4C spectrometer.

Concentrations of the $[Fe(SO_3CF_3)(H_2O)(TpivPP)]$ stock solutions were determined by using known extinction coefficients, while those of the NO_2^- solutions were determined by weighing. Ph_4PNO_2 was prepared as described previously,[1] weighed, and used directly. KNO_2 concentrations depended upon the concentration of 18-C-6. Excess solid KNO_2 was stirred with solutions of 18-C-6 of known concentrations determined by weighing.

Graphical analysis of the titration data was carried out with Cricket Graph software on a Macintosh II personal computer. Numerical fits were made by using the Los Alamos nonlinear least-squares program run on the Macintosh II computer. Weights used in the analysis were inversely proportional to nitrite concentration.

All NMR spectra were obtained on a Nicolet NT300 spectrometer operating at 300.063 MHz with a spectral bandwidth of ±30 kHz (±100 ppm) at the ambient temperature of 23 °C unless noted otherwise. All accumulations used 5-μs pulses followed by a 500-μs delay time. The number of FID accumulations varied from 500 to 5000. All spectra were referenced to the contaminant $CHCl_3$ of the $CDCl_3$ solvent, which was assigned at 7.24 ppm vs TMS. All solutions were prepared in $CDCl_3$ from a stock solution of $[Fe(SO_3CF_3)(H_2O)(TpivPP)]$. (Porphinato)iron(III) concentrations were in the range 1.63–4.1 mM.

Table I. Crystallographic Data for $[K(18\text{-}C\text{-}6)(H_2O)][Fe(NO_2)_2(TpivPP)]$

$FeKO_{15}N_{10}C_{76}H_{90}$	fw = 1478.56
a = 16.691 (6) Å	T = 293 K
c = 13.534 (3) Å	λ = 0.71073 Å
V = 3738.0 Å^3	μ = 0.324 mm^{-1}
Z = 2	$R(F_o)$ = 0.069
space group: $P\bar{4}$	$R_w(F_o)$ = 0.066

Structure Determination. A dark purple crystal of $[K(18\text{-}C\text{-}6)(H_2O)][Fe(NO_2)_2(TpivPP)]$ with approximate dimensions of 0.18 × 0.28 × 0.31 was mounted on the end of a glass fiber. Preliminary examination on a CAD4 diffractometer suggested a two-molecule tetragonal cell with final cell constants as reported in Table I. Complete crystallographic details (including data collection parameters) are given in Table SI. The systematic absences and Laue symmetry are consistent with three possible space groups: $P4$ (No. 75), $P\bar{4}$ (No. 81) and $P4/m$ (No. 83). Intensity data were measured at room temperature out to a maximum $2\theta = 68.2°$ by using graphite-monochromated Mo Kα radiation. Intensity data were reduced by using the Blessing suite of data reduction programs.[5] A total of 4185 observed data[6] were used in subsequent refinement calculations.

The structure was solved by a combination of Patterson and direct methods. The Patterson map had Fe–Fe, K–K, and Fe–K vectors that were most convincingly interpreted in terms of placing both metal ions on the same 2-fold axis of the space group $P\bar{4}$. Attempts to interpret the Patterson map in the other two possible space groups, $P4$ and $P4/m$, are much less satisfactory.[7] The choice of $P\bar{4}$ as the most probable space group was fully confirmed by all subsequent developments during structure solution and refinement. Most atoms of the porphinato ligand were found with the direct-methods program DIRDIF.[8] The remainder of the structure was found in subsequent difference Fourier syntheses. The axial nitrite ligands to iron and the axial water ligand to potassium are along the 2-fold axis. The 18-crown-6 and the porphinato core plane were found to be perpendicular to the 2-fold axis. Two significant disorder problems were encountered: the oxygen atoms of both nitrite ions are found in two alternate orientations, and the 18-crown-6 macrocycle is located in two different orientations that are approximately related by a 30° rotation about the 2-fold axis. Two equal population sets of oxygen atom positions were located; however, the concomitant two different orientations of the carbon atom backbone were not clearly resolved. In the final model, only one set of carbon positions and two sets of oxygen positions were used to describe the 18-crown-6 macrocycle.

(1) Finnegan, M. G.; Lappin, A. G.; Scheidt, W. R. *Inorg. Chem.*, preceding paper in this issue.
(2) Collman, J. P.; Gagne, R. R.; Halbert, T. R.; Marchon, J.-C.; Reed, C. A. *J. Am. Chem. Soc.* **1973**, *95*, 7868. Collman, J. P.; Gagne, R. R.; Reed, C. A.; Robinson, W. T.; Rodley, G. A. *Proc. Natl. Acad. Sci. U.S.A.* **1974**, *71*, 1326.
(3) Abbreviations used: $H_2TpivPP$, *meso*-$\alpha,\alpha,\alpha,\alpha$-tetrakis(*o*-pivalamidophenyl)porphyrin (picket-fence porphyrin); 18-C-6, 1,4,7,10,13,16-hexaoxacyclooctadecane (18-crown-6); Me_2-18-C-6, 2,6-dimethyl-18-crown-6; cryptand 222, 4,7,13,16,21,24-hexaoxa-1,10-diazabicyclo-[8.8.8]hexacosane (Kriptofix 222); DB-18-C-6, 2,3,11,12-dibenzo-1,4,7,10,13,16-hexaoxacyclooctadeca-2,11-diene.
(4) (a) Gismelseed, A.; Bominaar, E. L.; Bill, E.; Trautwein, A. X.; Winkler, H.; Nasri, H.; Doppelt, P.; Fisher, J.; Weiss, R. *Inorg. Chem.*, in press. (b) Nasri, H. Ph.D. Thesis, Univ. Louis Pasteur, Strasbourg, France, 1987.
(5) Blessing, R. H. *Crystallogr. Rev.* **1987**, *1*, 3.
(6) A total of 8337 data were measured. Because of the strong possibility that a noncentrosymmetric space group would be the correct choice for the space group, a number of $h,0,\pm l$ data were measured. A total of 226 such Freidel pairs were considered observed and are included in the 4184 observed data used in the structure analysis.
(7) The iron atoms in $P\bar{4}$ are placed on the 2-fold axes at 0, $^1/_2$, z and $^1/_2$, 0, $-z$, but would have to be placed at 0, $^1/_2$, z and $^1/_2$, 0, $+z$ in space group $P4$. Appropriate multiplicity sites in $P4/m$ require higher site symmetry (4 or $2/m$) that (a) fail to fit the observed vector distribution and (*b*) would also require substantial disorder.
(8) DIRDIF: Beurskens, P. T.; Bosman, W. P.; Doesburg, H. M.; Gould, R. O.; van den Hark, Th. E. M.; Prick, P. A. J.; Noordik, J. H.; Beurskens, G.; Parthasarathi, V.; Bruins Slot, H. J.; Haltiwanger, R. C.; Strumpel, M.; Smits, J. M. M. Technical Report 1984/1; Crystallography Laboratory: Nijmegen, The Netherlands, 1984. Other programs used in this study included local modifications of Jacobson's ALLS, Zalkin's FORDAP, Busing and Levy's ORFFE and ORFLS, and Johnson's ORTEP2. Atomic form factors were from: Cromer, D. T.; Mann, J. B. *Acta Crystallogr., Sect. A* **1968**, *A24*, 321. Real and imaginary corrections for anomalous dispersion in the form factor of the iron and potassium atoms were from: Cromer, D. T.; Liberman, D. J. *J. Chem. Phys.* **1970**, *53*, 1891. Scattering factors for hydrogen were from: Stewart, R. F.; Davidson, E. R.; Simpson, W. T. *J. Chem. Phys.* **1965**, *42*, 3175. All calculations were performed on a VAX 11/730 computer.

Table II. Fractional Coordinates for $[K(18\text{-C-6})(H_2O)][Fe(NO_2)_2(TpivPP)]$

atom	x	y	z
Fe	0.0000	0.5000	0.13857 (6)
K	0.0000	0.5000	−0.25399 (11)
O(1A)[a]	0.0572 (10)	0.5235 (12)	−0.0515 (10)
O(1B)[a]	−0.0145 (15)	0.5655 (15)	−0.0532 (16)
O(2A)[a]	−0.0566 (11)	0.4827 (18)	0.3304 (10)
O(2B)[a]	0.0170 (13)	0.4341 (12)	0.3350 (13)
O(3)	0.3851 (9)	0.4125 (9)	0.3375 (10)
O(4)	0.0778 (10)	0.8885 (8)	0.3474 (13)
N(1)	0.1001 (5)	0.4351 (6)	0.1371 (7)
N(2)	0.0661 (4)	0.5994 (4)	0.1390 (5)
N(3)	0.0000	0.5000	−0.0070 (4)
N(4)	0.0000	0.5000	0.2864 (4)
N(5)	0.2982 (6)	0.5099 (7)	0.3089 (7)
N(6)	−0.0172 (7)	0.7966 (7)	0.3135 (8)
C(a1)	0.1039 (6)	0.3510 (5)	0.1399 (7)
C(a2)	0.1799 (6)	0.4604 (7)	0.1413 (9)
C(a3)	0.1463 (6)	0.6056 (5)	0.1379 (7)
C(a4)	0.0375 (5)	0.6751 (5)	0.1371 (7)
C(b1)	0.1880 (7)	0.3280 (6)	0.1379 (9)
C(b2)	0.2312 (6)	0.3960 (7)	0.1396 (9)
C(b3)	0.1709 (7)	0.6873 (7)	0.1398 (9)
C(b4)	0.1046 (6)	0.7332 (6)	0.1406 (10)
C(m1)	0.2009 (6)	0.5441 (6)	0.1371 (9)
C(m2)	−0.0395 (6)	0.7013 (6)	0.1410 (7)
C(1)	0.2878 (7)	0.5570 (6)	0.1421 (9)
C(2)	0.3298 (7)	0.5931 (8)	0.0581 (8)
C(3)	0.4090 (6)	0.6071 (8)	0.0597 (11)
C(4)	0.4523 (7)	0.5900 (7)	0.1444 (11)
C(5)	0.4166 (6)	0.5607 (7)	0.2255 (7)
C(6)	0.3337 (6)	0.5429 (7)	0.2299 (9)
C(7)	0.3274 (8)	0.4516 (9)	0.3635 (9)
C(8)	0.2690 (10)	0.4254 (12)	0.4504 (13)
C(9)	0.2370 (16)	0.3437 (13)	0.4141 (16)
C(10)	0.2034 (11)	0.4752 (15)	0.4818 (18)
C(11)	0.3321 (15)	0.3932 (21)	0.5297 (16)
C(12)	−0.0617 (6)	0.7897 (5)	0.1406 (9)
C(13)	−0.0460 (7)	0.8356 (7)	0.2228 (8)
C(14)	−0.0612 (9)	0.9172 (8)	0.2247 (11)
C(15)	−0.0925 (7)	0.9527 (7)	0.1394 (9)
C(16)	−0.1069 (7)	0.9076 (8)	0.0585 (11)
C(17)	−0.0915 (7)	0.8237 (7)	0.0614 (9)
C(18)	0.0534 (11)	0.8226 (9)	0.3642 (13)
C(19)	0.0794 (8)	0.7777 (9)	0.4526 (10)
C(20)	0.1384 (17)	0.7076 (13)	0.4154 (16)
C(21)	0.0041 (15)	0.7199 (14)	0.4874 (13)
C(22)	0.0868 (19)	0.8222 (14)	0.5453 (16)
O(W)	0.0000	0.5000	−0.4544 (5)
O(5A)	−0.1139 (23)	0.3533 (13)	−0.2375 (23)
O(5B)	0.1631 (20)	0.5675 (15)	−0.1946 (13)
O(6A)	0.0570 (8)	0.3582 (6)	−0.1902 (13)
O(6B)	0.0197 (8)	0.6642 (8)	−0.2587 (12)
O(7A)	0.1692 (15)	0.4632 (16)	−0.2436 (19)
O(7B)	0.1321 (9)	0.4000 (7)	−0.2594 (15)
C(23)	−0.1759 (10)	0.3777 (10)	−0.2714 (13)
C(24)	−0.0804 (9)	0.3144 (9)	−0.1672 (10)

[a] Occupancy factors: O(1A), 0.57 (4); O(1B), 0.40 (3); O(2A), 0.59 (5); O(2B), 0.42 (4).

The structure was refined to convergence by using anisotropic temperature factors for all non-hydrogen atoms except the carbon atoms of the disordered 18-C-6. During the course of the refinement, a series of difference Fourier syntheses revealed approximate positions for all hydrogen atoms in the structure except the methyl hydrogens of the pickets and the methylene hydrogens of the 18-C-6. These hydrogen atoms were included as fixed contributors (C–H = 0.095 Å; $B(H) = 1.2B(C)$). The final model included 482 variables; the final cycle of full-matrix least-squares refinement had a largest parameter shift of 0.65 times its esd. At convergence, the final value of the unweighted R was 0.069 and that of the weighted R was 0.0659. The corresponding values for the opposite enantiomer were 0.069 and 0.0663. The original choice is marginally superior and is the one reported here. A final difference Fourier synthesis was judged free of significant features with the largest peak having a height of 0.43 e/Å^3. Final values of the atomic coordinates are listed in Table II, while the anisotropic thermal parameters and coordinates of the fixed parameters are included as supplementary material.

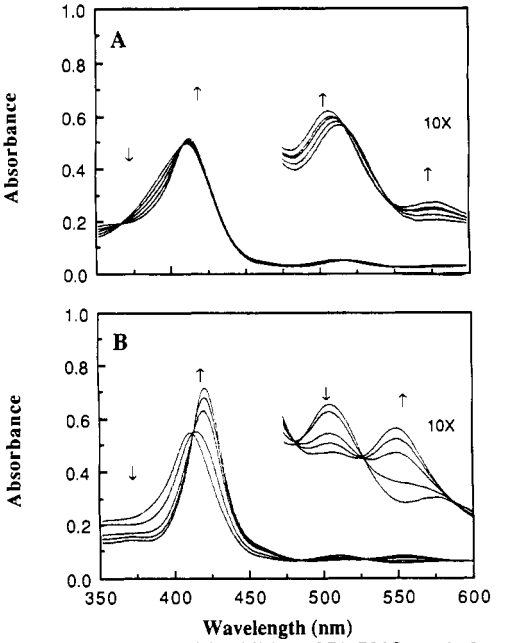

Figure 1. Spectral changes with addition of Ph_4PNO_2 to 6.12×10^{-5} M $[Fe(SO_3CF_3)(H_2O)(TpivPP)]$ in CH_2Cl_2 (0.1-cm length): (A) Fe/NO_2^- ratios up to 1:1 displayed; (B) Fe/NO_2^- ratios from 1:1 to 1:5 given.

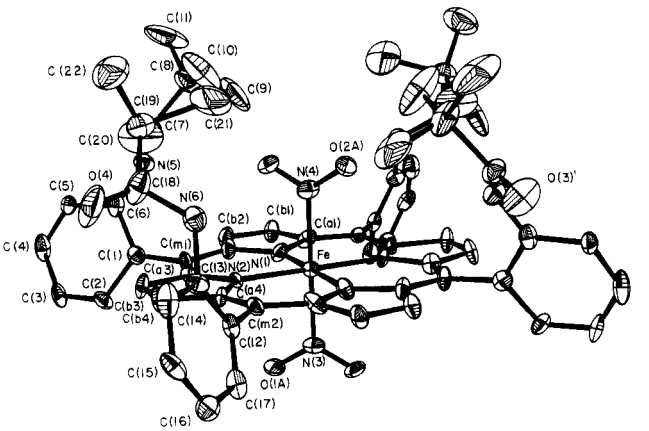

Figure 2. ORTEP diagram of the $[Fe(NO_2)_2(TpivPP)]^-$ showing the atom-labeling scheme used in all tables. The 30% probability ellipsoids are shown. Only one orientation of the nitrite ligands is shown.

Results and Discussion

The reaction of $[Fe(SO_3CF_3)(H_2O)(TpivPP)]$ with nitrite ion proceeds smoothly with several sources of nitrite as shown by visible spectroscopy (Figure 1). Solid complexes containing coordinated nitrite were obtained from reaction systems in which KNO_2 was solubilized by a crown (18-C-6) or cryptand (222) or by using Ph_4PNO_2. These compounds appear to have long-term stability in the solid state. Even in solution, the apparent stabilities of the complexes are significantly enhanced over those found in the preceding paper.[1] All picket-fence species are more stable in chlorobenzene solution compared to dichloromethane solution. Interestingly, the solution stabilities appear to have a significant counterion dependence, with the complexes prepared with Ph_4PNO_2 as the nitrite ion source being significantly less stable. As shown below, we believe that this effect may arise from the formation of an ion pair, especially for the case where the counterion is the $[K(18\text{-C-6})]^+$ complex.

The formulation of these species as nitrite complexes has been confirmed by the single-crystal X-ray structure determination of $[K(18\text{-C-6})(H_2O)][Fe(NO_2)_2(TpivPP)]$. The structure of the $[Fe(NO_2)_2(TpivPP)]^-$ anion is shown in Figure 2, which clearly shows the significant bonding features of the iron–nitrite ion interaction. The iron(III) atom is coordinated to two nitrite ions through the nitrogen atoms and forms a low-spin complex. The low-spin state is clearly suggested by the EPR g values (given in

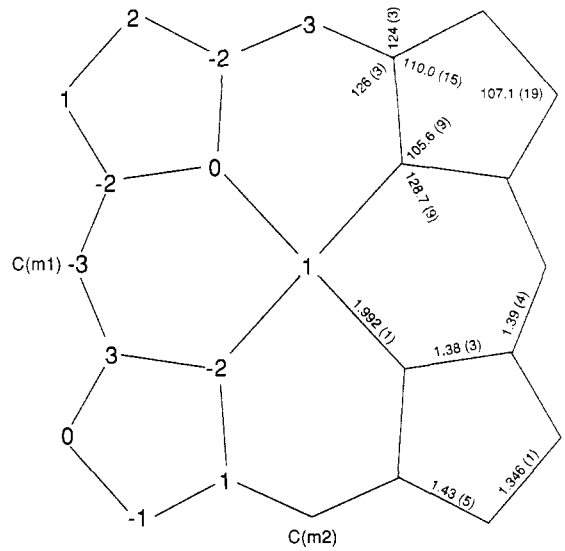

Figure 3. Formal diagram of the porphinato core in $[Fe(NO_2)_2(TpivPP)]^-$ displaying averaged values of bond distances and angles in the porphinato core and the displacement of the unique atoms (units of 0.01 Å) from the mean plane of the 24-atom core.

Table III. Bond Distances in $[K(18\text{-C-6})(H_2O)][Fe(NO_2)_2(TpivPP)]^a$

Fe–N(1)	1.991 (9)	C(7)–C(8)	1.589 (19)
Fe–N(2)	1.992 (7)	C(8)–C(9)	1.545 (28)
Fe–N(3)	1.970 (5)	C(8)–C(10)	1.439 (28)
Fe–N(4)	2.001 (6)	C(8)–C(11)	1.597 (25)
N(1)–C(a1)	1.406 (13)	C(12)–C(13)	1.376 (16)
N(1)–C(a2)	1.399 (13)	C(12)–C(17)	1.311 (17)
N(2)–C(a3)	1.344 (12)	C(14)–C(15)	1.398 (19)
N(2)–C(b4)	1.351 (12)	C(15)–C(16)	1.351 (20)
N(3)–O(1A)	1.196 (15)	C(16)–C(17)	1.423 (17)
N(3)–O(1B)	1.283 (24)	C(18)–C(19)	1.475 (21)
N(4)–O(2A)	1.153 (19)	C(19)–C(20)	1.610 (25)
N(4)–O(2B)	1.313 (19)	C(19)–C(21)	1.653 (27)
N(5)–C(6)	1.340 (16)	C(19)–C(22)	1.463 (25)
N(5)–C(17)	1.316 (16)	K–O(1A)	2.929 (14)
N(6)–C(13)	1.470 (16)	K–O(1B)	2.939 (23)
N(6)–C(18)	1.432 (19)	K–O(W)	2.712 (7)
C(a1)–C(b1)	1.456 (14)	K–O(5A)	3.108 (28)
C(a1)–C(m2)′	1.386 (13)	K–O(5B)	3.05 (3)
C(a2)–C(b2)	1.375 (15)	K–O(6A)	2.693 (11)
C(a2)–C(m1)	1.441 (14)	K–O(6B)	2.762 (14)
C(a3)–C(b3)	1.425 (13)	K–O(7A)	2.894 (24)
C(a3)–C(m1)	1.371 (13)	K–O(7B)	2.766 (13)
C(a4)–C(b4)	1.482 (12)	O(5A)–C(23)	1.20 (3)
C(a4)–C(m2)	1.359 (13)	O(5A)–C(24)	1.281 (26)
C(b1)–C(b2)	1.346 (16)	O(5B)–C(23)	1.401 (28)
C(b3)–C(b4)	1.345 (16)	O(5B)–C(28)	1.135 (28)
C(m1)–C(1)	1.468 (15)	O(6A)–C(25)	1.388 (18)
C(m2)–C(12)	1.521 (13)	O(6A)–C(26)	1.366 (23)
O(3)–C(7)	1.214 (18)	O(6B)–C(24)	1.639 (21)
O(4)–C(18)	1.195 (19)	O(6B)–C(25)	1.264 (19)
C(1)–C(2)	1.464 (15)	O(7A)–C(27)	1.078 (22)
C(1)–C(6)	1.433 (16)	O(7A)–C(28)	1.46 (3)
C(2)–C(3)	1.342 (15)	O(7B)–C(26)	1.288 (22)
C(3)–C(4)	1.385 (20)	O(7B)–C(27)	1.361 (20)
C(4)–C(5)	1.341 (17)	C(24)–C(25)	1.690 (22)
C(5)–C(6)	1.417 (15)	C(26)–C(27)	1.725 (22)

[a] Numbers in parentheses are estimated standard deviations in the least significant digit(s). Primed and unprimed symbols denote a pair of atoms related by the 2-fold axis.

the Experimental Section) with identical signals observed in powder and frozen solution and is corroborated by the coordination group distance parameters. The average Fe–N_p bond distance is 1.992 (1) Å, while the two axial Fe–$N(NO_2)$ distances are 2.001 (6) and 1.969 (5) Å. These distances are consistent with those expected[9] for a low-spin iron(III) porphyrinate. The axial bond

Table IV. Bond Angles in $[K(18\text{-C-6})(H_2O)][Fe(NO_2)_2(TpivPP)]^a$

N(1)FeN2)	89.3 (5)	O(3)C(7)N(5)	121.8 (12)
N(1)FeN(3)	89.4 (3)	O(3)C(7)C(8)	123.6 (13)
N(1)FeN(4)	90.6 (3)	N(5)C(7)C(8)	113.1 (12)
N(2)FeN(3)	90.2 (2)	C(7)C(8)C(9)	102.7 (15)
N(2)FeN(4)	89.8 (2)	C(7)C(8)C(10)	121.8 (14)
N(3)FeN(4)	180.00	C(7)C(8)C(11)	100.7 (14)
FeN(3)O(1A)	120.2 (7)	C(9)C(8)C(10)	109.9 (18)
FeN(3)O(1B)	119.2 (11)	C(9)C(8)C(11)	98.3 (20)
FeN(4)O(2A)	121.1 (8)	C(10)C(8)C(11)	119.9 (19)
FeN(4)O(2B)	120.1 (9)	C(13)C(12)C(m2)	119.4 (10)
FeN(1)C(a1)	125.5 (7)	C(17)C(12)C(m2)	121.0 (10)
FeN(1)C(a2)	129.4 (8)	C(13)C(12)C(17)	119.5 (9)
FeN(2)C(a3)	128.1 (6)	C(15)C(14)C(13)	117.9 (12)
FeN(2)C(a4)	125.7 (5)	C(16)C(15)C(14)	120.0 (11)
O(1A)N(3)O(1A)′	119.5 (15)	C(17)C(16)C(15)	119.6 (12)
O(1B)N(3)O(1B)′	121.7 (22)	C(16)C(17)C(12)	121.1 (12)
O(1A)N(3)O(1B)	68.0 (18)	C(14)C(13)C(12)	121.9 (11)
O(2A)N(4)O(2A)′	117.8 (16)	C(12)C(13)N(6)	119.3 (10)
O(2A)N(4)O(2B)	73.0 (19)	C(14)C(13)N(6)	118.7 (11)
O(2B)N(4)O(2B)′	119.8 (19)	C(18)N(6)C(13)	122.4 (12)
C(a1)N(1)C(a2)	104.9 (8)	O(4)C(18)N(6)	117.9 (16)
C(a3)N(2)C(a4)	106.2 (7)	O(4)C(18)C(19)	121.4 (15)
N(1)C(a1)C(m2)′	126.5 (9)	N(6)C(18)C(19)	118.5 (13)
N(1)C(a1)C(b1)	107.9 (8)	C(18)C(19)C(20)	107.2 (13)
C(b1)C(a1)C(m2)′	125.5 (8)	C(18)C(19)C(21)	107.7 (12)
N(1)C(a2)C(m1)	121.5 (10)	C(18)C(19)C(22)	117.6 (16)
N(1)C(a2)C(b2)	110.9 (10)	C(20)C(19)C(21)	97.5 (16)
C(b2)C(a2)C(m1)	127.3 (10)	C(20)C(19)C(22)	125.7 (17)
N(2)C(a3)C(m1)	127.2 (8)	C(21)C(19)C(22)	96.6 (15)
N(2)C(a3)C(b3)	111.2 (8)	O(w)KO(5A)	94.1 (6)
C(b3)C(a3)C(m1)	121.7 (9)	O(w)KO(5B)	105.2 (4)
N(2)C(a4)C(m2)	129.4 (8)	O(w)KO(6A)	108.7 (4)
N(2)C(a4)C(b4)	110.1 (8)	O(w)KO(6B)	88.7 (3)
C(b4)C(a4)C(m2)	120.2 (9)	O(w)KO(7A)	92.8 (5)
C(a1)C(b1)C(b2)	107.1 (9)	O(w)KO(7B)	88.5 (4)
C(a2)C(b2)C(b1)	109.0 (10)	O(5A)KO(5B)	31.2 (8)
C(a3)C(b3)C(b4)	107.9 (9)	O(5A)KO(6A)	60.1 (6)
C(a4)C(b4)C(b3)	104.5 (9)	O(5B)KO(6B)	62.2 (6)
C(a3)C(m1)C(a2)	124.3 (9)	O(6A)KO(6B)	34.6 (4)
C(1)C(m1)C(a2)	112.3 (9)	O(6A)KO(7A)	56.8 (6)
C(1)C(m1)C(a3)	123.1 (9)	O(6B)KO(7B)	59.7 (4)
C(a1)′C(m2)C(a4)	122.0 (8)	O(7A)KO(7B)	25.2 (7)
C(12)C(m2)C(a4)	122.9 (8)	O(7A)KO(5A)′	64.3 (7)
C(12)C(m2)C(a1)′	114.9 (9)	C(23)O(5A)C(24)	146 (4)
C(2)C(1)C(m1)	119.8 (10)	C(28)′O(5B)C(23)	73.5 (18)
C(6)C(1)C(m1)	122.8 (10)	C(25)O(6A)C(26)	102.2 (12)
C(2)C(1)C(6)	117.1 (10)	C(24)O(6B)C(25)	69.8 (11)
C(3)C(2)C(1)	122.1 (11)	C(27)O(7A)C(28)	117.4 (29)
C(4)C(3)C(2)	119.4 (12)	C(26)O(7B)C(27)	81.2 (14)
C(5)C(4)C(3)	121.4 (10)	O(5A)C(23)C(28)′	122.5 (19)
C(6)C(5)C(4)	122.9 (10)	O(5A)C(24)C(25)	110.4 (23)
C(5)C(6)N(5)	123.4 (10)	O(6A)C(25)C(24)	103.7 (12)
C(1)C(6)N(5)	119.6 (10)	O(6A)C(26)C(27)	104.8 (12)
C(1)C(6)C(5)	116.9 (10)	O(7A)C(27)C(26)	107.1 (21)
C(7)N(5)C(6)	126.1 (11)	O(7A)C(28)C(23)′	127.7 (17)

[a] Numbers in parentheses are the estimated standard deviation in the least significant digit(s). Primed and unprimed symbols denote a pair of atoms related by 2-fold axis.

distances are comparable to but perhaps shorter than the 2.008 (6) Å found for the Fe–$N(NO_2)$ distance in a nitrosyl(nitro)iron dithiocarbamate complex,[10] the only other iron example we find for such a distance. The difference in the two axial Fe–$N(NO_2)$ bond distances is surprising. The shorter Fe–$N(NO_2)$ distance involves the nitrite ion that also interacts with the potassium ion. It might have been expected that this potassium ion interaction might weaken the interaction with iron and lead to a longer bond, contrary to observation. The nitrite ion in the ligand-binding pocket does not hydrogen bond to the amide hydrogen atoms, the other obvious phenomenon that might affect the Fe–$N(NO_2)$ bond distance.

Figure 3 is a formal diagram of the porphinato core. Although the uncertainties in individual values are relatively large, the

(9) Scheidt, W. R.; Reed, C. A. *Chem. Rev.* **1981**, *81*, 543.

(10) Ileperuma, O. A.; Feltham, R. D. *Inorg. Chem.* **1977**, *16*, 1876.

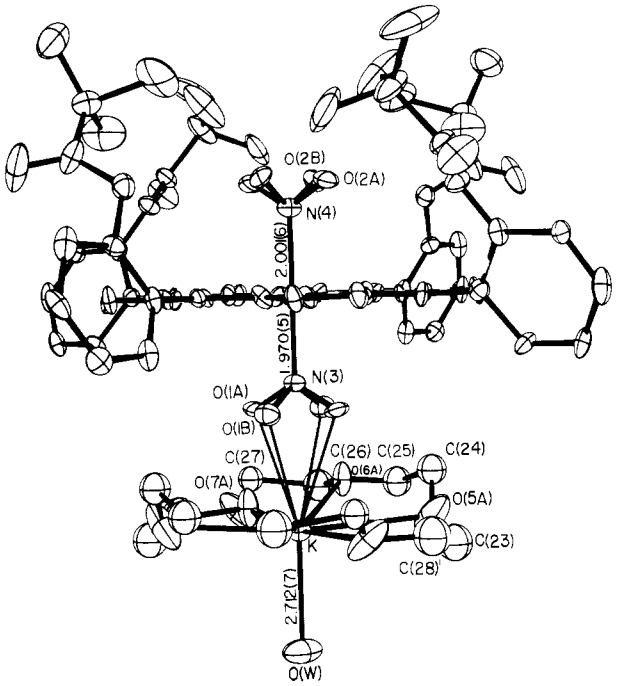

Figure 4. ORTEP diagram of $[K(18\text{-}C\text{-}6)(H_2O)][Fe(NO_2)_2(TpivPP)]$, showing the close approach of $[K(18\text{-}C\text{-}6)(H_2O)]^+$ to the exposed nitrite ion. The required 2-fold symmetry axis is along the axial Fe–N(NO_2) bonds and the axial K–O(H_2O) bond. Both orientations of the two disordered nitrite ions are shown. Also given in the figure is the labeling scheme for the unique atoms of the cation and the disordered nitrite ions.

average values are within expectations. Individual values of bond distances and angles in the porphinato core and in the $[K(18\text{-}C\text{-}6)(H_2O)]^+$ cation are given in Tables III and IV, respectively. Also displayed in Figure 3 are the deviations (in units of 0.01 Å) of each unique atom from the mean plane of the 24-atom core. The porphinato core is effectively planar with the iron(III) atom centered in the hole in the four porphyrin nitrogen atoms.

Figure 4 displays a most interesting feature of the $[K(18\text{-}C\text{-}6)(H_2O)][Fe(NO_2)_2(TpivPP)]$ species, the interaction of the $[K(18\text{-}C\text{-}6)(H_2O)]^+$ cation with the $[Fe(NO_2)_2(TpivPP)]^-$ anion. This diagram is an edge-on view showing the two faces of the porphyrin core. Figure 4 clearly shows how structural features of the $[K(18\text{-}C\text{-}6)(H_2O)][Fe(NO_2)_2(TpivPP)]$ system can substantially hinder any interaction between coordinated nitrite and a free nitrite ion. One coordinated nitrite ion is, as expected, quite protected by the pocket provided by the pivalamide pickets. Surprisingly, the remaining nitrite ion, coordinated to the "open" face of the porphyrin species, also appears to be protected against such reaction by the relatively close interaction of the nitrite oxygen atoms with the potassium ion. The potassium ion coordinates to both oxygen atoms of the nitrite ion with a unique K–O distance of 2.929 (14) Å. The alternate nitrite ion orientation forms a similar K–O distance of 2.939 (23) Å. Thus, these interactions between the potassium and oxygen are actually within observed K–O bonding distances. Especially cogent examples are the K–O distances in potassium-*nitrate* complexes of DB-18-C-6[11] and Me_2-18-C-6.[12] In these complexes, the K–O(NO_3) distances to bidentate nitrate are 2.73–2.86 Å. These eight-coordinate complexes have the potassium ion displaced toward the *sole* axial ligand, the bidentate nitrate ion. In the current case, the potassium ion is actually displaced on the opposite side of the 18-C-6 plane toward the water axial ligand. We thus describe the environment of potassium ion in $[K(18\text{-}C\text{-}6)(H_2O)][Fe(NO_2)_2(TpivPP)]$ as nine-coordinate with a hexagonal girdle and three axial ligand interactions. The equatorial bonding features of the potassium ion with the 18-crown-6 macrocycle appear normal.[13,14] The mean planes of the porphyrin and 18-C-6 macrocycles are parallel to each other as required by the 2-fold symmetry of the two planes. If the notion that the above K(18-C-6) protective structure is responsible for the reduced reactivity of coordinated nitrite in solution, it would require that this protective structure remain intact in solution. We have no direct evidence for this, but the differences in details of ligand-binding equilibria and solution NMR as a function of the counterion are consistent with this. Interestingly, Dyer et al.[12] believe that the solution and solid-state structure are essentially equivalent in the potassium nitrate complex of Me_2-18-C-6.

Figure 4 also shows another structural feature of interest: the relative orientation of the nitro ligands. We have shown for bis(imidazole) complexes[15] that the electronic structure of iron(III) is sensitive to the relative orientation of the two imidazole planes; paralllel ligand plane orientations yield normal b-type hemichrome EPR spectra while perpendicular orientations give the so-called strong g_{max} spectrum. Since the nitrite ion, like imidazole, should be a good π donor, we would expect a similar correlation. Unfortunately we are unable to be completely certain whether the two nitro ligand planes have parallel or perpendicular relative orientations because of the disorder in these two axial ligands. The crystallographic data (populations of the two orientations) suggest that the two ligands exist in the parallel configuration (to within 5°), an observation in accord with the "normal" rhombic EPR spectrum observed.

The molecular structure of $[K(18\text{-}C\text{-}6)(H_2O)][Fe(NO_2)_2(TpivPP)]$ suggested that the nitrite ion coordinated to the "open" face of the picket-fence porphyrin derivative had a significant, strong interaction with the $[K(18\text{-}C\text{-}6)]^+$ counterion. As noted above, we believe that this should at least be described as a tight ion pair. Because of this anticipated ionic interaction between $[K(18\text{-}C\text{-}6)]^+$ and $[Fe(Tpiv)(NO_2)_2]^+$, two sets of titrations with $[Fe(SO_3CF_3)(H_2O)(TpivPP)]$ were done in order to compare the possible effects of the counterion. The two different salts used as sources of nitrite ion were Ph_4PNO_2 and $[K(18\text{-}C\text{-}6)]NO_2$. Both sets of titrations were done in dichloromethane. Small but reproducible differences in the dependence of the absorbance spectra upon nitrite concentration in these titrations with the two salts appear to show counterion effects attributable to differences either in ion-pair formation per se or in its effect upon the stability constants. Moreover, while CH_2Cl_2 solutions $[K(18\text{-}C\text{-}6)(H_2O)][Fe(NO_2)_2(TpivPP)]$ appeared stable over a period of several days, the corresponding solutions of $Ph_4P[Fe(TpivPP)(NO_2)_2]$ decompose to give [Fe(TpivPP)Cl] in the span of a few hours, consistent with differences in stabilization of the bis(nitrite) species by ionic interactions in the solution phase.

In CH_2Cl_2 solution with Ph_4P^+ and $[K(18\text{-}C\text{-}6)]^+$ as the respective counterions, the formation of the mono(nitrite) and bis(nitrite) species appears to follow a stepwise association with the differences attributable to ion-pairing effects. The appearance

(11) Battaglia, L. P.; Corradi, A. B.; Bianchi, A.; Giusti, J.; Paoletti, P. *J. Chem. Soc., Dalton Trans.* **1987**, 1779.

(12) Dyer, R. B.; Ghiradellis, R. G.; Palmer, R. A.; Holt, E. M. *Inorg. Chem.* **1986**, *25*, 3184.

(13) Thirteen structures of K(18-C-6) complexes (without serious disorder) found[14] in the Cambridge Crystallographic Data Base have a range of K–O distances between 2.62 and 3.10 Å.

(14) Liotta, C. L.; McLaughlin, M. L.; Vanderveer, D. G.; O'Brien, B. A. *Tetrahedron Lett.* **1984**, *25*, 1665. Bandy, J. A.; Berry, A.; Green, M. L. H.; Perutz, R. N.; Prout, K.; Verpeaux, J.-N. *J. Chem. Soc., Chem. Commun.* **1984**, 729. Miravitilles, C.; Molins, E.; Solans, X.; Germain, G.; Declercq, J. P. *J. Inclusion Phenom.* **1985**, *3*, 27. Walker, J. A.; Knobler, C. B.; Hawthorne, M. F. *Inorg. Chem.* **1985**, *24*, 2688. Egorov, M. P.; Bel'skii, V. K.; Petrov, E. S.; Terekhova, M. I.; Beletskaya, I. P. *Zh. Org. Khim* **1984**, *20*, 2033. Rath, N. P.; Holt, E. M. *J. Chem. Soc., Chem. Commun.* **1986**, 311. Schmidpeter, A.; Burget, G.; Zwaschka, F.; Sheldrick, W. S. *Z. Anorg. Allg. Chem.* **1985**, *527*, 17. Horwitz, C. P.; Holt, E. M.; Brock, C. P.; Shriver, D. F. *J. Am. Chem. Soc.* **1985**, *107*, 8136. von Seyerl, J.; Scheidsteger, O.; Berke, H.; Huttner, G. *J. Org. Chem.* **1986**, *311*, 85. Balletti, A. M. R.; Braca, G.; Sbrana, G.; Marchetti, F. *J. Mol. Catal.* **1985**, *32*, 291. Wang, M.; Zheng, P.; Zheng, J.-I.; Zhong, C.; Shen, J.-M. Yang, Y.-H. *Acta Crystallogr., Sect. C* **1987**, *C43*, 1544. Carl, R. T.; Hughes, R. P.; Johnson, J. A.; Davis, R. E.; Kashyap, R. P. *J. Am. Chem. Soc.* **1988**, *110*, 603. Barnes, J. C.; Collard, J. *Acta Crystallogr., Sect. C* **1988**, *C44*, 565.

(15) Walker, F. A.; Huynh, B. H.; Scheidt, W. R.; Osvath, S. F. *J. Am. Chem. Soc.* **1986**, *108*, 5288.

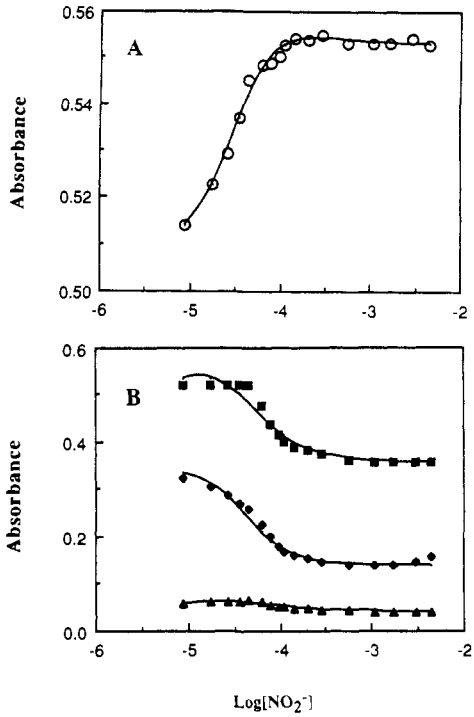

Figure 5. Titrations of $[Fe(SO_3CF_3)(H_2O)(TpivPP)]$ with $[K(18\text{-}C\text{-}6)]NO_2$ in CH_2Cl_2, with fits determined by least-squares analysis according to eq 3: (A) absorbance values at 415.2 nm with values of K_1, K_2 and ϵ_{ML} fitted as given in text; (B) absorbance values at 408.0 (■), 383.5 (◆), and 507.2 (▲) nm. Conditions are as in Figure 1. Least-squares fits were obtained from fits of ϵ_{ML} with values of $(2.2 \pm 0.1) \times 10^5$, $(7.9 \pm 0.8) \times 10^4$, and $(3.1 \pm 0.1) \times 10^4$ M^{-1} cm^{-1}, respectively.

of the spectral titration of $[NO_2^-]$ with $[Fe(SO_3CF_3)(H_2O)(TpivPP)]$ suggested that K_1 and K_2, the constants for NO_2^- association, are both large and comparable in magnitude. Attempts to extract values of K_1 and ϵ_{ML} from these titration data by a graphical method[16] were made by constructing linearized plots of $1/(A - A_0)$ vs $1/[NO_2^-]$ according to

$$1/(A - A_0) = 1/(K_1(A_1 - A_0)[NO_2^-]) + 1/(A_1 - A_0) \quad (1)$$

The values for $K_1 = 1.49 \times 10^4$ M^{-1} and $\epsilon_{ML} = 1.24 \times 10^4$ M^{-1} cm^{-1} (507 nm) were obtained for the Ph_4PNO_2 titration. These values were used in the plots according to

$$(A_0 - A)/A[NO_2^-]^2 + (A_1 - A)K_1/A[NO_2^-] = K_1K_2 - K_1K_2A_2/A \quad (2)$$

to determine $K_2 = 4.0 \times 10^4$ M^{-1} and $\epsilon_{ML_2} = 6.6 \times 10^3$ M^{-1} cm^{-1}. The closeness of the equilibrium constants and the inherent uncertainty in this type of calculation (where all three species exist in the system at nearly all concentrations of ligand) led to an attempt to fit the data numerically to the equation given by Rossotti.[16]

$$A/[M]_0 = (\epsilon_M + \epsilon_{ML}[NO_2]K_1 + \epsilon_{ML}[NO_2]_2K_1K_2)/(1 + K_1[NO_2] + K_1K_2[NO_2]_2) \quad (3)$$

Data at 415.2 nm were used to fit the three parameters K_1, K_2 and ϵ_{ML}. Vallues of $\epsilon_M = 8.286 \times 10^4$ M^{-1} cm^{-1} and $\epsilon_{ML_2} = 9.036 \times 10^4$ M^{-1} cm^{-1} were available from spectra of $[Fe(SO_3CF_3)(H_2O)(TpivPP)]$ alone and under high NO_2^- concentrations, respectively, and were held fixed. Values of $K_1 = (4 \pm 1) \times 10^3$ M^{-1}, $K_2 = (1.81 \pm 0.03) \times 10^5$ M^{-1}, and $\epsilon_{ML} = (1.1 \pm 0.1) \times 10^5$ M^{-1} cm^{-1} were obtained. This fit is shown in Figure 5A. The general consistency of K_1 and K_2 thus obtained were checked by applying them to spectral data at 383.3, 408.0 and 507.2 nm. Values for ϵ_{ML} were calculated at each of these wavelengths; the resulting fits are shown in Figure 5B.

A similar computational treatment for the $[K(18\text{-}C\text{-}6)]^+$ titration data gave $K_1 = (5.1 \pm 0.8) \times 10^3$ M^{-1} and $K_2 = (9 \pm 3) \times 10^3$ M^{-1}, which again was confirmed at the various wavelengths. Calculated ϵ_{ML} values did not differ significantly from those obtained with Ph_4P^+ as the counterion. The calculated K_1 value for the two titrations is within experimental error, but the values of K_2 clearly differ by an order of magnitude. We believe that these association constant differences can be interpreted in structural terms. The similar K_1 values suggest that the first nitrite binds in the picket-fence pocket (similar environments) while the second nitrite must bind on the open face where environmental effects (such as ion pairing) can be maximized.

We have also done NMR titrations in an attempt to define the nature of the intermediate nitrite complex. The reaction of $[Fe(SO_3CF_3)(H_2O)(TpivPP)]$ and various amounts of nitrite, added either as Ph_4PNO_2 or as KNO_2 solubilized by using 18-C-6, was examined; the pyrrole β-proton signal was monitored. The NMR spectrum of $[Fe(SO_3CF_3)(H_2O)(TpivPP)]$ alone gives an $H_{pyrrole}$ signal at 31.7 ppm vs TMS.[17] The position of this peak shows a small temperature variation, shifting to 29.8 ppm at −40 °C. Addition of Ph_4PNO_2, even at concentrations less than that of iron porphyrin, results in the disappearance of the 31.7 ppm signal and the appearance of a signal at −15.7 ppm. The addition of more nitrite simply increased the intensity of the −15.7 ppm peak; no evidence of any line broadening or sharpening was seen over the entire range of nitrite additions. Decreasing the temperature of −40 °C did not give any new spectral features. However, when $[K(18\text{-}C\text{-}6)]NO_2$ was used as the nitrite source, initial additions gave a new peak at +75 ppm as well as the original 31.7 ppm signal. Further additions of nitrite lead to an increase in the intensity of the +75 ppm peak and a decrease in the 31.7 resonance until at $Fe/NO_2^- \sim 1$, a new resonance at −14.5 ppm appears which replaces the 31.7 ppm resonance. The low-spin peak increases in intensity without shifting (with concomitant decreases in the +75 ppm resonance) until it is the only pyrrole β-proton resonance. Thus the second NMR titration with $[K(18\text{-}C\text{-}6)]NO_2$ indicates that the mono(nitrite) species has a high-spin state. The differences in the NMR spectra in the intermediate nitrite concentration regime are consistent with the counterion dependence of K_2 (and constant K_1) since the low-spin bis(nitrite) complex signal is first seen at relatively lower concentration of Ph_4PNO_2 than of $[K(18\text{-}C\text{-}6)]NO_2$. Moreover, only the first system shows a signal for the intermediate species. Of course, limiting spectra for both titrations are consistent with a low-spin state for the bis(nitro) complex.

Another approach that was used to investigate the nature of the intermediate species was that of EPR. $[Fe(SO_3CF_3)(H_2O)(TpivPP)]$ (frozen chlorobenzene solution, 77 K) displays an axial spectrum with $g = 5.1$. Initial additions of nitrite ion (solubilized by using 18-C-6) causes a shift in the axial spectrum towards higher g. Subsequent additions lead to a decrease in the intensity of the high g signal, and eventually only the rhombic spectrum characteristic of the bis(nitro) complex is seen. We take the shift in the $g = 5.1$ signal to result from the production of a new high-spin species (g value near 6). Finally we note that the appearance[4,18] of the 507-nm band in the spectral titration data is also consistent with a high-spin intermediate.

The present work demonstrates that stable, isolable (nitro)(porphinato)iron(III) complexes can be prepared if the interaction between coordinated nitrite and free nitrite can be hindered. The aproach here for a bis(nitro) anionic complex makes use of a porphyrin pocket plus protection by ion-pair formation. The question of whether these bis(nitro) complexes will be useful

(16) Rossotti, F. J. C.; Rossotti, C. H. *Determination of Stability Constants*; McGraw-Hill: New York, 1961.

(17) Goff reports a larger temperature dependence for the β-pyrrole resonances for the analogous TPP complex: Boersma, A. D.; Goff, H. M. *Inorg. Chem.* **1982**, *21*, 581.

(18) Bounab, B. Ph.D. Thesis, Univ. Louis Pasteur, Strasbourg, France, 1985. UV–visible spectra of five-coordinate high-spin iron(III) picket-fence derivatives of the bromide, fluoride, chloride, iodide, acetate, and azide are reported in these theses. These spectral/spin-state correlations are also found for TPP derivatives.

synthetic intermediates in the preparation of other nitrite-containing complexes, e.g. five-coordinate or mixed-axial-ligand species, is under active investigation.

Acknowledgment. We thank the National Institutes of Health for support of this work through Grant GM-38401-16.

Supplementary Material Available: Table SI (complete crystallographic information), Table SII (anisotropic thermal parameters), and Table SIII (fixed atomic coordinates and thermal parameters for the hydrogen atoms) (4 pages); a listing of observed and calculated structure amplitude data (×10) (14 pages). Ordering information is given on any current masthead page.

Contribution from the Department of Chemistry,
The University of Michigan, Ann Arbor, Michigan 48109

Binucleating Macrocyclic [14]N_4 Ligands and Their Complexes. Synthesis of the Free Ligand 2,3-Dioxo-5,6:13,14-dibenzo-9,10-(4′,5′-dimethylbenzo)-1,4,8,11-tetraazacyclotetradeca-7,11-diene (L) and of the 7,12-Me_2-L Metal Complexes and Derivatives. Crystal Structures and Properties of the [M′][M(7,12-Me_2-L)] Complexes (M = Ni(II); M = Co(II); M′ = $ZnCl_2$, M = Ni(II); M′ = $[Na(5\text{-crown-}15)]^+$, M = Ni(II); M′ = $[(C_2H_5)_4N]^+$, M = Ni(II))

D. Christodoulou, M. G. Kanatzidis, and D. Coucouvanis*

Received April 17, 1989

The free macrocyclic ligand 2,3-dioxo-5,6:13,14-dibenzo-9,10-(4′,5′-dimethylbenzo)-1,4,8,11-tetraazacyclotetradeca-7,11-diene, abbreviated α-diketo-TAD-Me_2, and its complexes with Ni(II) and Co(II) have been synthesized. The Ni(II) complex readily undergoes reduction and by virtue of the α-diketone function, appended to the macrocyclic ring, can bind to other metal ions. Complexes of the 2,3-dioxo-5,6:13,14-dibenzo-7,12-dimethyl-9,10-(4′,5′-dimethylbenzo)-1,4,8,11-tetraazacyclotetradeca-7,11-diene, abbreviated α-diketo-TAD-Me_4, also have been synthesized. The structures of Ni(α-diketo-TAD-Me_4) (IVa), of the reduction derivatives (Et_4N)[Ni(α-diketo-TAD-Me_4+H)] (V) and [Na(5-crown-15)][Ni(α-diketo-TAD-Me_4+H)] (VI), and of the binuclear complex [Ni(α-diketo-TAD-Me_4)]$ZnCl_2$ (VII) are reported. Crystals of IVa are orthorhombic, space group *Pnam*; a = 7.934 (4) Å, b = 12.663 (6) Å, and c = 20.922 (9) Å. Crystals of V are monoclinic, space group $P2_1/a$; a = 14.789 (6) Å, b = 17.582 (5) Å, c = 15.372 (6) Å, and β = 108.36 (3)°. Crystals of VI are monoclinic, space group $P2_1/n$; a = 17.201 (11) Å, b = 12.113 (11) Å, c = 17.426 (12) Å, and β = 75.32 (5)°. Crystals of VII are monoclinic, space group $P2_1/c$; a = 11.139 (9) Å, b = 16.19 (2) Å, c = 16.15 (1) Å, and β = 98.03 (7)°. Refinements by full-matrix least squares of 151 parameters on 1085 data for IVa, of 371 parameters on 2455 data for V, of 349 parameters on 2440 data for VI, and of 215 parameters on 1514 data for VII converged to the R values of 0.044, 0.073, 0.078, and 0.073, respectively. In all structures the hydrogen atoms were included in the structure factor calculations but were not refined. In IVa the macrocycle adopts a saddle-shaped conformation and the molecules stack along the crystallographic a axis. The planar NiN_4 chromophores are equally spaced with a Ni-Ni distance of 4.059 (1) Å. In V and VI the reduction has resulted in the saturation of one of the imino bonds, and in the structure of VI the Na^+ ion is coordinated by the α-diketo function and is found at 5.070 (9) Å from the Ni atom. In VII the Zn atom also is coordinated by the α-diketo function and is located 5.140 (3) Å from the Ni atom. The electrochemistry and electronic spectra of the complexes are reported. Co(α-diketo-TAD-Me_2), which is a high-spin, square-planar Co(II) complex, shows a quasireversible reduction at −0.86 V vs SCE and binds O_2 reversibly.

Introduction

A rapidly emerging area of chemical interest in recent years concerns the synthesis of heterobinucleating ligands and the coordination chemistry of the heteronuclear complexes that derive from such ligands. Examples of heterobinucleating ligands that could serve as "polytopic receptor molecules"[1] for the binding of metal cations, or the cobinding of metal ions and molecular substrates, include molecules that contain macrocyclic (polyether) functionalities appended to porphyrin[1] or *N,N′*-ethylenebis(salicylideneaminato)[2] (salen) centers, phenols appended to macrocyclic tetraamines,[3] and aromatic phosphines appended to the acetylacetonate anion.[4]

In addition to the employment of specifically designed ligand systems as mentioned above, heterometallic complexes have been obtained also in reactions where metal complexes are used as ligands for various Lewis acids. In these reactions, the availability of more than one lone pair on a donor atom, or of multiple donor atoms within a coordinated ligand, introduce the potential for second-order interactions that under appropriate conditions lead to heteronuclear aggregates. Included in this class are complexes derived from metal cyanides,[5] metal thiocyanates,[6] $(\eta^5\text{-}C_5H_5)_2M(SR)_2$ complexes (M = Ti,[7] Mo,[8] W,[8] Nb[9]), $(\eta^5\text{-}C_5H_5)_2Zr(PPh_2)_2$ complexes,[10] salen complexes,[11,12] the tetrathiometalate anions,

(1) Hamilton, A.; Lehn, J. M.; Sessler, J. L. *J. Am. Chem. Soc.* **1986**, *108*, 5158-5167.
(2) van Staveren, C. J.; Reinhoudt, D. N.; van Eerden, J.; Harkema, S. *J. Chem. Soc., Chem. Commun.* **1987**, 974-977.
(3) Kimura, E.; Koike, T.; Uenishi, K.; Hediger, M.; Kuramoto, M.; Joko, S.; Arai, Y.; Kodama, M.; Iitaka, Y. *Inorg. Chem.* **1987**, *26*, 2975-2983.
(4) Wrobleski, D.; Rauchfuss, T. B. *J. Am. Chem. Soc.* **1982**, *104*, 2314-2316.
(5) Ludi, A.; Gudel, H. U. *Struct. Bonding* **1973**, *14*, 1.
(6) Armor, J. N.; Haim, A. *J. Am. Chem. Soc.* **1971**, *93*, 867.
(7) (a) Braterman, P. S.; Wilson, V. A. *J. Organomet. Chem.* **1971**, *31*, 131. (b) Braterman, P. S.; Wilson, V. A.; Joshi, K. K. *J. Organomet. Chem.* **1971**, *31*, 123. (c) Dias, A. R.; Green, M. L. H. *Rev. Port. Quim.* **1969**, *11*, 61.
(8) Dias, A. R.; Green, M. L. H. *J. Chem. Soc. A* **1971**, 1951.
(9) Douglas, W. E.; Green, M. L. H. *J. Chem. Soc., Dalton Trans.* **1972**, 1796.
(10) (a) Gelmini, L.; Stephan, D. W. *Inorg. Chem.* **1986**, *25*, 1222-1225. (b) Gelmini, L.; Matassa, L. C.; Stephan, D. W. *Inorg. Chem.* **1985**, *24*, 2585-2588.
(11) (a) Sinn, E.; Harris, C. M. *Coord. Chem. Rev.* **1969**, *4*, 391. (b) Hobday, M. D.; Smith, T. D. *Ibid.* **1972**, *9*, 311. (c) Bear, C. A.; Waters, J. M.; Waters, T. N. *J. Chem. Soc., Dalton Trans.* **1974**, 1059. (d) Gruber, S. J.; Harris, C. M.; Sinn, E. *J. Inorg. Nucl. Chem.* **1968**, *30*, 1805.

0020-1669/90/1329-0191$02.50/0